Biogeosciences Discuss., 11, 2887–2932, 2014
www.biogeosciences-discuss.net/11/2887/2014/
doi:10.5194/bgd-11-2887-2014

Biogeosciences
Discussions
Open Access

Carbon cycle uncertainty in the Alaskan Arctic

J. B. Fisher[1], M. Sikka[1], W. C. Oechel[2], D. N. Huntzinger[3], J. R. Melton[4], C. D. Koven[5], A. Ahlström[6], A. M. Arain[7], I. Baker[8], J. M. Chen[9], P. Ciais[10], C. Davidson[11], M. Dietze[12], B. El-Masri[13], D. Hayes[14], C. Huntingford[15], A. Jain[13], P. E. Levy[16], M. R. Lomas[17], B. Poulter[10], D. Price[18], A. K. Sahoo[19], K. Schaefer[20], H. Tian[21], E. Tomelleri[22], H. Verbeeck[23], N. Viovy[10], R. Wania[24], N. Zeng[25], and C. E. Miller[1]

[1]Jet Propulsion Laboratory, California Institute of Technology, 4800 Oak Grove Drive, Pasadena, CA, 91109, USA
[2]Global Change Research Group, Department of Biology, San Diego State University, San Diego, CA, 92182, USA and the Fondazione Edmund Mach, San Michele all'Adige (TN), 38010, Italy
[3]School of Earth Sciences and Environmental Sustainability, Northern Arizona University, P.O. Box 5694, Flagstaff, AZ, 86011, USA
[4]Canadian Centre for Climate Modelling and Analysis, Environment Canada, Victoria, BC, V8W 2Y2, Canada
[5]Earth Sciences Division, Lawrence Berkeley National Laboratory, Berkeley, CA, 94708, USA
[6]Department of Physical Geography and Ecosystem Science, Lund University, Sölvegatan 12, 223 62, Lund, Sweden

[7]School of Geography and Earth Sciences, McMaster University, 1280 Main Street West, Hamilton, Ontario, L8S 4K1, Canada
[8]Atmospheric Science Department, Colorado State University, Fort Collins, CO, 80523-1371, USA
[9]Department of Geography, University of Toronto, 100 St. George Street, Toronto, Ontario, M5S 3G3, Canada
[10]Laboratoire des Sciences du Climat et l'Environnement, Orme des Merisiers, bat. 701 – Point courier 129, 91191 Gif Sur Yvette, France
[11]Program in Ecology, Evolution, and Conservation Biology, University of Illinois at Urbana-Champaign, 505 S. Goodwin Ave, Urbana, IL, 61801, USA
[12]Department of Earth and the Environment, Boston University, 675 Commonwealth Ave, Boston, MA, 02215, USA
[13]Department of Atmospheric Sciences, University of Illinois, Urbana, IL, 61801, USA
[14]Climate Change Science Institute and Environmental Sciences Division, Oak Ridge National Laboratory, Oak Ridge, TN, 37831-6301, USA
[15]Centre for Ecology and Hydrology, Benson Lane, Wallingford, OX10 8BB, UK
[16]Centre for Ecology and Hydrology, Penicuik, Midlothian, EH26 0QB, UK
[17]Centre for Terrestrial Carbon Dynamics, University of Sheffield, Dept. of Animal and Plant Sciences, Western Bank, Sheffield, S10 2TN, UK
[18]Natural Resources Canada, Northern Forestry Centre, 5320-122 Street Northwest, Edmonton, Alberta, T6H 3S5, Canada
[19]Department of Civil and Environmental Engineering, Princeton University, Princeton, New Jersey, 08544, USA
[20]National Snow and Ice Data Center, Cooperative Institute for Research in Environmental Sciences, University of Colorado at Boulder, Boulder, CO, 80309, USA
[21]School of Forestry and Wildlife Sciences, Auburn University, 602 Duncan Drive, Auburn, AL, 36849, USA
[22]Biogeochemical Model-Data Integration Group, Max Planck Institute for Biogeochemistry, Hans-Knöll-Str. 10, 07745, Jena, Germany
[23]Laboratory of Plant Ecology, Faculty of Bioscience Engineering, Ghent University, Coupure Links 653, 9000 Ghent, Belgium

BGD
11, 2887–2932, 2014

[24]Institut des Sciences de l'Evolution (UMR5554, CNRS), Université Montpellier 2, Place Eugène Bataillon, 34090 Montpellier, France
[25]Department of Atmospheric and Oceanic Science, University of Maryland, 2417 Computer and Space Sciences Building, College Park, MD, 20742–2425, USA

Received: 22 January 2014 – Accepted: 30 January 2014 – Published: 20 February 2014

Correspondence to: J. B. Fisher (jbfisher@jpl.nasa.gov)

Published by Copernicus Publications on behalf of the European Geosciences Union.

Abstract

Climate change is leading to a disproportionately large warming in the high northern latitudes, but the magnitude and sign of the future carbon balance of the Arctic are highly uncertain. Using 40 terrestrial biosphere models for Alaska, we provide a baseline of terrestrial carbon cycle structural and parametric uncertainty, defined as the multi-model standard deviation (σ) against the mean ($\overline{x}$) for each quantity. Mean annual uncertainty ($\sigma/\overline{x}$) was largest for net ecosystem exchange (NEE) ($-0.01 \pm 0.19\,kg\,C\,m^{-2}\,yr^{-1}$), then net primary production (NPP) ($0.14 \pm 0.33\,kg\,C\,m^{-2}\,yr^{-1}$), autotrophic respiration (Ra) ($0.09 \pm 0.20\,kg\,C\,m^{-2}\,yr^{-1}$), gross primary production (GPP) ($0.22 \pm 0.50\,kg\,C\,m^{-2}\,yr^{-1}$), ecosystem respiration (Re) ($0.23 \pm 0.38\,kg\,C\,m^{-2}\,yr^{-1}$), CH_4 flux ($2.52 \pm 4.02\,g\,CH_4\,m^{-2}\,yr^{-1}$), heterotrophic respiration (Rh) ($0.14 \pm 0.20\,kg\,C\,m^{-2}\,yr^{-1}$), and soil carbon ($14.0 \pm 9.2\,kg\,C\,m^{-2}$). The spatial patterns in regional carbon stocks and fluxes varied widely with some models showing NEE for Alaska as a strong carbon sink, others as a strong carbon source, while still others as carbon neutral. Additionally, a feedback (i.e., sensitivity) analysis was conducted of 20th century NEE to CO_2 fertilization (β) and climate (γ), which showed that uncertainty in γ was 2x larger than that of β, with neither indicating that the Alaskan Arctic is shifting towards a certain net carbon sink or source. Finally, AmeriFlux data are used at two sites in the Alaskan Arctic to evaluate the regional patterns; observed seasonal NEE was captured within multi-model uncertainty. This assessment of carbon cycle uncertainties may be used as a baseline for the improvement of experimental and modeling activities, as well as a reference for future trajectories in carbon cycling with climate change in the Alaskan Arctic.

1 Introduction

Changes in climate have led to a relatively large warming in the high northern latitudes, i.e., the Arctic, due to a temperature–albedo feedback from the loss of snow and sea ice, as well as the breakdown of polar near-surface temperature inversions (i.e., more water vapor, leading to greater greenhouse gas effect; also, changes in cloud cover) (Cess et al., 1991; Chapin et al., 2005; Chapman and Walsh, 1993, 2007; IPCC, 2007; McGuire et al., 2006; Overpeck et al., 1997; Serreze et al., 2000; Walsh et al., 2002). Throughout the Holocene, Arctic ecosystems have absorbed more CO_2 from the atmosphere through photosynthesis than have emitted back to the atmosphere through respiration (Kuhry et al., 2009; Marion and Oechel, 1993; Oechel et al., 1993; Ping et al., 2008; Tarnocai, 2006). The pervasive cold and wet conditions in the Arctic have limited the decay of soil organic carbon, resulting in the accumulation of carbon on the order of 35–70 $kg\,C\,m^{-2}$ total (~ 25 % of the global soil organic carbon pool; Mishra and Riley, 2012; Ping et al., 2008; Tarnocai et al., 2009) stored beneath the permafrost and in peatlands over centuries to millennia.

Warming, however, is thawing permafrost, resulting in the release of previously stored soil carbon to the atmosphere, thereby exacerbating the atmospheric CO_2 impact on climate (Belshe et al., 2013, 2012; Burke et al., 2012; Christensen et al., 2004; Hayes et al., 2011; Koven et al., 2011; McGuire et al., 2009; Natali et al., 2012, 2013; Oechel et al., 1993, 2000; Oechel and Vourlitis, 1994; Schaefer et al., 2011; Schuur and Abbott, 2011; Schuur et al., 2013, 2008, 2009; Zimov et al., 2006). Alternatively, warming accelerates soil decomposition, which may release nutrients into the nutrient-limited ecosystems, and, combined with more favorable growing conditions and additional growing days, drive the Arctic towards a carbon sink regime (Mack et al., 2004; Qian et al., 2010; Sistla et al., 2013). However, there are currently no large-scale observations of the Arctic net ecosystem exchange (NEE) of CO_2, and it is therefore not now possible to determine with certainty whether or not the Arctic is a net carbon sink or source, let alone the future Arctic CO_2 flux magnitude or even sign of flux (Hinzman et al., 2005; McGuire et al., 2009, 2012).

A number of new field campaigns aim to address these uncertainties: the Carbon in Arctic Reservoirs Vulnerability Experiment (CARVE) (Miller et al., 2010); the Arctic Boreal Vulnerability Experiment (ABoVE) (Goetz et al., 2011); and, the Next Gener-

BGD
11, 2887–2932, 2014

ation Ecological Experiment (NGEE Arctic) (Wullschleger et al., 2011). All of these campaigns include Alaska as a major region of focus, with aims of reducing uncertainty in the Arctic carbon cycle. However, the uncertainty itself is uncertain, i.e., the uncertainty has not been well quantified. McGuire et al. (2012) recently compiled the most extensive suite of data and models for the Arctic to date, but this included only three terrestrial biosphere models (TBMs), whereas the number of models driving uncertainty values in global climate change projections, for instance, is more on the order of dozens (Friedlingstein et al., 2006; IPCC, 2007).

Recent terrestrial biosphere model intercomparison projects (MIPs) – TRENDY (Piao et al., 2013), the North American Carbon Program (NACP) Regional and Site Syntheses (Hayes et al., 2012; Huntzinger et al., 2012; Schwalm et al., 2010), and the Wetland and Wetland CH_4 Inter-comparison of Models Project (WETCHIMP) (Melton et al., 2013; Wania et al., 2013) – have organized a multitude of international modeling teams to contribute their latest model estimates using both common forcing data (i.e., TRENDY; NACP Site) as well as a mixture of different forcing data (i.e., NACP Regional; WETCHIMP). The science community has been focused on diagnoses of individual model skill, benchmarking, and suggestions for improvements, so we avoid that here (Huntzinger et al., 2012; Schaefer et al., 2012; Schwalm et al., 2010). Here, we use the between-model variability from these MIPs to define the uncertainties in the Alaskan Arctic carbon cycle, specifically the structural and parametric representation of land surface physics as well as the forcing data. The objective of this analysis is to compile and quantify the predictive uncertainty in terrestrial carbon cycle dynamics applied to the Alaskan Arctic.

BGD
11, 2887–2932, 2014

2 Methods

2.1 Regional level

We used 14 NACP Regional Synthesis models, 9 TRENDY models, and 7 WETCHIMP models for regional carbon flux and/or stock estimates.

The 14 NACP Regional Synthesis models include (Table 1): BEPS (Chen et al., 1999), CanIBIS (El Maayar et al., 2002), CASA-GFED (van der Werf et al., 2004), CASA-TRANSCOM (Randerson et al., 1997), CLM-CASA (Randerson et al., 2009), CLM4-CN (Thornton et al., 2007), DLEM (Tian et al., 2010), ISAM (Jain and Yang, 2005), LPJwsl (Sitch et al., 2003), MOD17 (Zhao et al., 2005), ORCHIDEE (Krinner et al., 2005), SiB3 (Baker et al., 2008), TEM6 (Hayes et al., 2011), and VEGAS2 (Zeng et al., 2005). Model output for the NACP Regional Synthesis was downloaded from: ftp://nacp.ornl.gov/synthesis/2008/firenze/continental/1_continental_data_model_inventory.html.

The 9 TRENDY models include: CLM4-CN (Thornton et al., 2007), HYLAND (Levy et al., 2004), LPJwsl (Sitch et al., 2003), LPJ-GUESS (Smith et al., 2001), OCN (Zaehle et al., 2010), ORCHIDEE (Krinner et al., 2005), SDGVM (Cramer et al., 2001), TRIFFID (Clark et al., 2011), and VEGAS (Zeng et al., 2005). Model output for TRENDY was downloaded from: http://www-lscedods.cea.fr/invsat/RECCAP/. Output from multiple versions of the same model were sometimes available; in these cases, we used output only from the most recent version. We primarily used the version S2 runs, which correspond to simultaneously meteorological forcings and atmospheric CO_2 concentration variation following 20th century increases, with disturbance turned off and a constant land use mask. We also used version S1, which varies only CO_2, to evaluate sensitivities to CO_2 and climate.

The 7 WETCHIMP models include: CLM4Me (Riley et al., 2011), DLEM (Tian et al., 2010), LPJ-Bern (Spahni et al., 2011), LPJ-WHyMe (Wania et al., 2010), LPJwsl (Sitch et al., 2003), ORCHIDEE (Krinner et al., 2005), and SDGVM (Cramer et al., 2001). Model output for WETCHIMP was downloaded from: http://arve.epfl.ch/

BGD
11, 2887–2932, 2014

pub/wetchimp. Output from six experiments were available (Melton et al., 2013), but we used only experiment 2, corresponding to the transient simulation from 1901–2009 using observed climate and CO_2 values.

Variables assessed for NACP Regional and TRENDY included: net ecosystem exchange (NEE), gross primary production (GPP), heterotrophic respiration (Rh), autotrophic respiration (Ra), net primary production (NPP), and soil carbon stock (Csoil). Some models provided GPP and NPP, but not Ra, while others provided GPP and Ra, but not NPP, so we were able to calculate the missing term in those equations with one unknown. CH_4 was provided from only WETCHIMP models, and this is solely for what we used the WETCHIMP models. Most variables were identical across NACP Regional and TRENDY, except that the net CO_2 flux was reported as net biome production (NBP) for TRENDY (and, net ecosystem production, NEP, for HYLAND only), whereas oppositely it was reported as NEE for NACP Regional. We reversed the sign for TRENDY (and converted time units of seconds to months) to equate the CO_2 flux between both MIPs, though we note that technically NBP should include additional fluxes from fire and other disturbances as well as lateral carbon transport that NEE would not include. LPJwsl and VEGAS from TRENDY were not converted because their values were already in the units of NACP. HYLAND and SDGVM in TRENDY were reported in incorrect sign so we reversed the sign.

We created a half-degree resolution mask of Alaska and a mask of the North Slope (Fig. 1) used to clip from the global (TRENDY) and N. America (NACP Regional) model output. We transformed the masks to match the different native resolutions of the models. We produced mean annual maps for Alaska for NEE, GPP, Rh, Ra, NPP, and Csoil by averaging the available monthly model output and preserving the native spatial resolution for each model. We set a uniform color scale bar for between-model visual comparison (rather than individual scale bars for each model, which would highlight within-model spatial variability). However, in some the range was effectively truncated due to some large values beyond our set min/max of the scale; in other cases the

BGD
11, 2887–2932, 2014

min/max was wider than a given model's range so spatial variation within that model may be difficult to visualize.

We produced maps for the multi-model mean ($\overline{x}$) and standard deviation (σ) from the individual mean annual maps. Given non-uniform spatial resolutions across models, we present the multi-model and σ at the finest resolution (i.e., 0.5°). We arithmetically downscaled all models with coarser resolutions to 0.5°. Pixels that overlapped with one another across models were used to calculate the individual half-degree pixel averages. Finally, we re-applied the half-degree mask of Alaska to the resultant multi-model $\overline{x}$ and σ maps (i.e., removing newly-added beyond-coastal pixels from the combination of some wider-extent, coarse scale models). The multi-model color scale bar was set equal to that of the individual model maps; the color scale bar for the σ was set differently, tailored to the range of the σ. We also generated a time series plot from the spatial mean of all pixels in the Alaskan Arctic for each month for each model (except for Csoil, which did not vary temporally over our time domain).

While the MIPs enable us to conduct an extensive analysis, they also impose some limitations, which must be caveated: (i) not all possible TBMs are included in the MIPs (e.g., there are TBMs used in the science community that were not contributed); (ii) the models are not completely independent from one another, at times sharing similar physics for some processes, and with some contributing to multiple MIPs; (iii) the forcing data accuracy and variability were not assessed (though they were originally cross-checked and considered the best available); and, (iv) some models have more sophisticated representation of the biophysical processes important in the Arctic than others (though all TBMs provide Arctic estimates). Nonetheless, the data available for this analysis provide a representative range of information to calculate a baseline of uncertainty and variability in key environmental variables of the Alaskan Arctic. Overcoming some of the above limitations would allow improvements in the estimation of our baseline uncertainty.

To assess the model sensitivity of the terrestrial carbon cycle, we follow the "Feedback analysis" approach of Friedlingstein et al. (2006) and Cox et al. (2013) for their

BGD
11, 2887–2932, 2014

uncoupled simulations. That is, the change in land carbon storage sensitivity to change in atmospheric CO_2 concentration may be formulated as:

$$\Delta C_L^{u,A} = \beta_L \Delta C_A^u \tag{1}$$

where ΔC_L^u is the change in land carbon storage in the uncoupled simulation arising from an increase in atmospheric CO_2 concentration of ΔC_A^u, and β_L is the land carbon sensitivity to atmospheric CO_2. Friedlingstein et al. use Eq. (1) to show the cumulative absolute change in land carbon storage from each of the uncoupled C^4MIP runs against atmospheric CO_2 concentration for uncoupled simulations, which we also follow. To isolate the impact from "climate change", Friedlingstein et al. give the following equation, which we adapt from their coupled runs:

$$\Delta C_L^{u,A+T} = \beta_L \Delta C_A^u + \gamma_L \Delta T^c \tag{2}$$

where γ_L is the land carbon sensitivity to climate change with temperature increase of ΔT^c. Subtracting Eq. (1) from Eq. (2):

$$\gamma_L = \Delta C_L^{clim} / \Delta T^c \tag{3}$$

which can isolate the "climate alone" impact on land carbon uptake, where ΔC_L^{clim} is the change in land carbon from climate alone. The resultant analysis shows the cumulative net CO_2 flux over the 20th century as the σ between the TRENDY models forced with CO_2 alone (e.g., TRENDY version S1), forced with varying CO_2 + climate (e.g., TRENDY version S2), and the difference between the two, which is the impact of climate alone. NACP models were not used for the feedback analysis because NACP output was not provided over the 20th century.

2.2 Site level

We used model output from 10 NACP Site Synthesis models, which include: CanIBIS (El Maayar et al., 2002), CNCLASS (Arain et al., 2006), DLEM (Tian et al., 2010),

BGD
11, 2887–2932, 2014

Ecosys (Grant et al., 2009), LPJwsl (Sitch et al., 2003), ORCHIDEE (Krinner et al., 2005), SiB (Baker et al., 2008), SiBCASA (Schaefer et al., 2008), SSiB2 (Xue et al., 1991), and TECO (Weng and Luo, 2008). Model output for the NACP Site Synthesis was downloaded from: http://isynth-site.pbworks.com/w/page/9422807/FrontPage. Models were provided with in situ measured forcing data for each site to produce site level (e.g., point) model estimates.

In situ data from the Alaskan North Slope Atqasuk (70.4696° N, −157.4089° W) and Barrow (71.3225° N, −156.6259° W) sites (Kwon et al., 2006) (Fig. 1) were downloaded from: http://www.fluxdata.org (Agarwal et al., 2010). The in situ sites are part of the regional AmeriFlux network and global FLUXNET network where tower-based eddy covariance fluxes and micrometeorological variables are measured (Baldocchi, 2008). Half-hourly data were used to compute mean diurnal (from mean hourly) and seasonal (from mean monthly) cycles.

Atqasuk consists of moist-wet coastal sedge tundra and moist-tussock tundra surfaces (e.g., *Eriophorum vaginatum*) in the well-drained upland. Barrow consists of undisturbed wet-moist coastal sedge tundra types, multiple ice wedges, drained lake tundra land forms, and is located 2 km south of the Arctic Ocean and 100 km north of Atqasuk; Barrow was not heavily glaciated during the last period of glaciation. Atqasuk's more continental climate and sandy substrate make a useful contrast with conditions at Barrow (Kwon et al., 2006). Another Alaskan ground site, Ivotuk, was operational; however, site-level model simulations were not available for this site.

To maintain consistency for fair comparisons, when one data point was missing for either model or site, we removed all data points for that time step for all models and measurements; thus, the averages shown are not necessarily "true" averages for each model or measurements. Days were excluded if fewer than 12 h of data were available. We used the available in situ data to define our site level time domain: 2003–2006 for Atqasuk; and, 1998–2002 for Barrow. In situ data for Barrow were available only during the growing season (northern summer) for most years. Variables assessed included: NEE, GPP, Re, and Csoil. NACP processed files for NEE, GPP, and Re were used for

BGD
11, 2887–2932, 2014

analysis; original/raw NetCDF (nc) files were used for all other variables. Raw files for ORCHIDEE had to be time shifted by 9 h; leap years were adjusted for ORCHIDEE and LPJwsl. Not all models or sites provided data for all variables. Models did not provide diurnally or seasonally varying site level Csoil so analysis of Csoil was done at the annual timescale only.

To link the site measurements to the regional model patterns, we evaluated the correlation structure between NEE and GPP or Re at the sites vs. the region. That is, we calculated the r^2 for NEE vs. GPP and NEE vs. Re. This was done for the site measurements and for each model at the regional level. We then evaluated how well the regional models matched the site level correlation patterns.

To provide a spatial picture of how representative the sites are to the larger region, we constructed statewide site representativeness maps based on statewide spatially explicit climatology using the Incremental Analysis Updates (IAU) 2d atmospheric single level diagnostics (near surface air temperature) and IAU 2d land surface diagnostics (precipitation) from the Modern Era Retrospective analysis for Research and Applications (MERRA) generated by NASA's Global Modeling and Assimilation Office (GMAO) at $0.5^{\circ} \times 0.66^{\circ}$ resolution (Rienecker et al., 2011). MERRA data were downloaded from: http://disc.sci.gsfc.nasa.gov/daac-bin/DataHoldings.pl?LOOKUPID_List=MAT1NX*** (where *** is "SLV" or "LND" for air temperature and precipitation, respectively). We compared the mean daily time series of site level air temperature and precipitation for 2001 (i.e., the year that both sites overlapped, for comparison; flux data were not available at Atqasuk for 2001) against the corresponding time series of the MERRA data for each pixel in Alaska, computing the correlation coefficient (r^2) for each pixel (e.g., variability representativeness). We removed MERRA data for time steps where there were data gaps from the in situ data. We adjusted the time zones between the in situ data and MERRA (i.e., Alaskan Standard Time, AST; and, Greenwich Mean Time, GMT, respectively) to match. We converted units of air temperature from Kelvin (MERRA) to Celsius (in situ), and of precipitation from mm (in situ) to $\mathrm{kg\,m^{-2}\,s^{-1}}$ (MERRA) to match.

BGD
11, 2887–2932, 2014

3 Results

The results are partitioned into 5 sub-sections: (i) spatial variability; (ii) temporal variability; (iii) an integrated summary; (iv) sensitivity analysis; and, (v) site level evaluation.

3.1 Spatial variability in carbon

The spatial patterns in mean annual NEE for Alaska varied widely among the models, essentially showing no consistency, with almost all patterns having at least one other model showing the opposite pattern (Fig. 2; data for a single year, 2003, are shown for example, though these relative patterns remain for other years). Some models showed the entire region as a strong carbon sink, others as a strong carbon source, while still others as close to carbon neutral. Some models showed a large portion of the region as a carbon sink with the rest of the state a carbon source; other models showed the opposite pattern of source and sink distribution. It is also visually apparent that the spatial resolutions vary widely among models (i.e., $0.5^{\circ} \times 0.5^{\circ}$–$2.5^{\circ} \times 3.75^{\circ}$). The multi-model mean annual NEE for Alaska shows the region as largely carbon neutral (Fig. 3a). The multi-model annual NEE σ for Alaska shows model agreement or disagreement distributed throughout the region, with greater agreement in boreal regions than in tundra regions (Fig. 3b).

We provide in the Supplement the same spatial diagnostics for the carbon components that comprise NEE – that is, GPP, NPP, Rh, and Ra (Figs. S1–S8).

For CH_4, fluxes were primarily present and largest in the southern-most regions of Alaska (Figs. 4 and 5a). Most model disagreement was along the southwest Alaska Peninsula and southeast Alaska Panhandle (Fig. 5b). There was also significant disagreement as to whether or not CH_4 fluxes occur at all in the interior of Alaska. Models such as DLEM and ORCHIDEE estimated no interior CH_4 flux; whereas, LPJ-WHyME, LPJ-Bern, and SDGVM estimated moderate to high fluxes of CH_4. The spatial differences in CH_4 fluxes among models are primarily due to differences in wetland location schemes in the models, and the magnitude of the fluxes due to the vegetation dynam-

BGD
11, 2887–2932, 2014

ics and soil maps used in the models (Olefeldt et al., 2013). LPJ-WHyME and LPJ-Bern both used a peatland database to determine peatland locations (the two models also contain similar code structures), which gives them CH_4-producing regions more centrally, though they are not identical because of differences in inundation thresholds and wet mineral soils leading to CH_4 fluxes. DLEM, ORCHIDEE, LPJwsl, and CLM4Me all ingest or are parameterized from an inundation dataset, which provided a bias away from interior CH_4-producing regions. SDGVM calculates the wetlands extent independently, somewhat similar to the process in LPJ-Bern.

Total soil carbon for the Alaskan Arctic (North Slope) varied from 1.4 to 29.3 $kg\,C\,m^{-2}$ across models (Fig. 6), with a multi-model mean of 14.0 $kg\,C\,m^{-2}$ and σ of 9.2 $kg\,C\,m^{-2}$. We provide the spatial diagnostics for soil carbon in Supplement Figs. S9 (individual models) and S10 (multi-model mean and standard deviation). There was no clear spatial pattern similarity across models in soil carbon, with the greatest multi-model uncertainty throughout the permafrost areas in the north.

3.2 Temporal variability in carbon

The mean Alaskan Arctic time-varying NEE for each model was generally similar in timing across models, showing carbon sinks in the growing season, separated by small carbon sources in the winter (Fig. 7; we show two years for comparison, 2002–2003, though the relative patterns remain for other years). The multi-model de-trended (from the multi-model mean) σ was 0.01 $kg\,C\,m^{-2}\,yr^{-1}$. The multi-model mean month of greatest CO_2 uptake was July, with a σ of 0.5 months.

We provide in the Supplement the same time series plots for the carbon components that comprise NEE (GPP, NPP, Rh, and Ra; Figs. S11–S14). Of particular note is the considerable variability among models in their estimates of Rh during the winter (November–March) (Fig. S13), when all other flux components minimized to zero during this “dormant” period (i.e., November–March). This pattern was corroborated by a recent analysis of winter Rh (between 0–20 % of annual Rh) in similar ecosystems

BGD
11, 2887–2932, 2014

(Wang et al., 2011). The winter carbon source is also seen as integrated into the time series of NEE in Fig. 7.

The time series for CH_4 showed similar temporal patterns for most of the models with CH_4 flux emissions year round for many models (Fig. 8). The multi-model mean month of greatest CH_4 emission was August for both years, with a σ of 1.4 months. The variability in timing of greatest CH_4 emission was nearly 3x that of greatest CO_2 uptake, indicating large uncertainty in CH_4 flux timing relative to that of CO_2, presumably because the climatic controls on photosynthesis (light and temperature) constrain the period of greatest CO_2 uptake more narrowly than the combination of temperature and soil moisture that would be likely to affect the modeled seasonal maximum CH_4 release.

Seasonal patterns were negligible for soil carbon (e.g., relatively constant throughout each year) so these are not shown.

3.3 Summary of carbon uncertainties

From a total carbon perspective, the largest quantity of absolute σ is in soil carbon, followed by GPP, Re, NPP, Ra = Rh, NEE, and CH_4. However, σ tends to scale with $\overline{x}$ magnitude, so we also evaluate $\sigma/\overline{x}$ (Fig. 9). The largest relative (as opposed to absolute) uncertainty was in NEE at 2100 % ($-0.01 \pm 0.19\,\mathrm{kg\,C\,m^{-2}\,yr^{-1}}$), followed by NPP at 233 % ($0.14 \pm 0.33\,\mathrm{kg\,C\,m^{-2}\,yr^{-1}}$), Ra at 226 % ($0.09 \pm 0.20\,\mathrm{kg\,C\,m^{-2}\,yr^{-1}}$), GPP at 225 % ($0.22 \pm 0.50\,\mathrm{kg\,C\,m^{-2}\,yr^{-1}}$), Re at 169 % ($0.23 \pm 0.38\,\mathrm{kg\,C\,m^{-2}\,yr^{-1}}$), CH_4 flux at 160 % ($2.52 \pm 4.02\,\mathrm{g\,CH_4\,m^{-2}\,yr^{-1}}$), Rh at 149 % ($0.14 \pm 0.20\,\mathrm{kg\,C\,m^{-2}\,yr^{-1}}$), and soil carbon at 66 % ($14.0 \pm 9.2\,\mathrm{kg\,C\,m^{-2}}$). The exceptionally large $\sigma/\overline{x}$ for NEE is primarily because is a small number; nonetheless, σ tends to scale with $\overline{x}$ magnitude – in the case of NEE it did not. The absolute σ of NEE is on the same order as that from the other non-CH_4 carbon flux components (0.2 vs. 0.20–$0.50\,\mathrm{kg\,C\,m^{-2}\,yr^{-1}}$); but, because NEE $\overline{x}$ is a much smaller number than the other flux components, the relative uncertainty is necessarily large. Conversely, the σ of soil carbon is large – $9.2\,\mathrm{kg\,C\,m^{-2}}$ – but,

BGD
11, 2887–2932, 2014

Title Page
Abstract | Introduction
Conclusions | References
Tables | Figures
Back | Close
Full Screen / Esc
Printer-friendly Version
Interactive Discussion

so too is the $\overline{x}$ (14.0 $kg\,C\,m^{-2}$), therefore the relative uncertainty for soil carbon is small compared to the other carbon components. It is expected that the uncertainty in NEE would dominate all carbon component uncertainties because NEE is the integration of multiple carbon components, so errors necessarily propagate and amplify. The relative uncertainty in NEE is approximately one order of magnitude greater (10x) than all other uncertainties.

3.4 Feedback/sensitivity analysis

We conducted a feedback/sensitivity analysis of 20th century NEE to CO_2 fertilization (β) and climate (γ) using the 9 TRENDY models. We accumulated NEE over time, and show and report the multi-model standard deviation at the end of the 20th century (i.e., 1901–2010). CO_2 fertilization alone drives the Alaskan Arctic towards a net carbon sink, though the uncertainty is still within the range of a net carbon source (Fig. 10a). The uncertainty in the climate-only impact is much larger than the uncertainty in the CO_2 fertilization impact – uncertainty in γ is 1.9x that of β – and there is no agreement as to whether or not climate is driving the Alaskan Arctic towards a net carbon sink or source (Fig. 10b). The combined effect of β and γ is dominated by the uncertainty in γ, and the resultant feedback analysis is that there is no consensus on whether or not the Alaskan Arctic is becoming a carbon sink or source (Fig. 10c and d).

3.5 Site level evaluation

For comparison to measurements, we present results from two sites located in the North Slope of Alaska – Atqasuk and Barrow – where a subset of models (NACP Site) were run using in situ forcing data to compare against measured carbon fluxes and soil carbon stocks. First, to understand how representative the sites were to the larger region in lieu of a comprehensive spatial sampling study, we conducted a comparison of climatology at each site to that in each pixel encompassing all of Alaska (Fig. S15). The expectation was that pixels closer to the sites would exhibit greater similarity in climatol-

BGD
11, 2887–2932, 2014

ogy, and this similarity would degrade following some linear or non-linear pattern within increasing distance away from the sites. Variability in climate was better represented in Atqasuk than Barrow relative to the wider region, which reinforces the conclusion that Atqasuk represents a more continental climate than does Barrow (Kwon et al., 2006).

Relative to in situ measured NEE, models did not capture the seasonal cycle well at either site (Fig. 11a and b). Nonetheless, observed NEE tended to be contained within the multi-model uncertainty, which gives some indication that the regional uncertainty (e.g., Fig. 7) may also capture the true signal of NEE. The mean model seasonal r^2 was: 0.07 at Atqasuk, and 0.50 at Barrow (both site mean: 0.29). The mean model seasonal RMSE was more similar than the r^2 between sites, with 0.44 $\mu mol\,CO_2\,m^{-2}\,s^{-1}$ at Atqasuk, and 0.46 $\mu mol\,CO_2\,m^{-2}\,s^{-1}$ at Barrow (both site mean: 0.45 $\mu mol\,CO_2\,m^{-2}\,s^{-1}$). The multi-model monthly mean NEE and σ were $-0.03 \pm 0.64\,\mu mol\,CO_2\,m^{-2}\,s^{-1}$ at Atqasuk, and $-0.4 \pm 0.54\,\mu mol\,CO_2\,m^{-2}\,s^{-1}$ at Barrow.

The greatest observed CO_2 uptake at Atqasuk was typically in June, whereas the multi-model mean placed the greatest CO_2 uptake in July. For Barrow, the month of greatest observed CO_2 uptake was typically July or August, and the multi-model mean tended to capture that timing accurately. This evaluation may extend into the regional analysis, indicating that the models likely capture the peak seasonal NEE timing, though possibly with a slight time lag. It is noted that the "observed" data presented here are not necessarily accurate representations of the actual in situ patterns because of our data-removal rule matching models to data (see Sect. 2 Methods).

To understand how well the regional models capture the dynamics partitioning NEE into GPP and Re, we evaluated the factorial correlation structure between these carbon fluxes at the site level, and compared that structure to the same correlation structure for each model at the regional level (North Slope). NEE at both sites was more correlated with GPP (0.49) than with Re (0.20), with the correlation being 2.5x greater for GPP than Re. Across all regional models, the multi-model mean NEE-to-GPP r^2 (0.77) was also larger than that for NEE-to-Re (0.50) by 1.6x, indicating the models were able to

BGD
11, 2887–2932, 2014

capture the differences in NEE partitioning between GPP and Re at the regional level along a similar partitioning structure as that at the site level, though the models had stronger NEE correlations with both GPP and Re, and not as much separation.

4 Discussion

The objective of this analysis was to compile and quantify predictive uncertainty in terrestrial carbon cycle dynamics for the Alaskan Arctic. Using a large sampling of terrestrial process models for the region, we evaluated the uncertainties contributing to divergent model results, and the resultant multi-model variability in carbon flux/stock estimation. We also evaluated the climate (γ) and CO_2 fertilization (β) sensitivities of ecosystem carbon dynamics, as well as patterns at the site level in the Alaskan Arctic against the regional patterns of the North Slope. These results are fundamental to future research in the Alaskan Arctic that can build on to reduce uncertainties in the Arctic carbon cycle.

While uncertainty in carbon fluxes dominated, there was also significant disagreement in modeled soil carbon stocks, suggesting a major area of focus for model development given the potential impact of mobilized Arctic soil carbon with climate change (Billings et al., 1982; Burke et al., 2012; Christensen et al., 2004; Hayes et al., 2011; Koven et al., 2011; McGuire et al., 2009; Oechel et al., 1993, 1997; Oechel and Vourlitis, 1994; Schaefer et al., 2011; Schuur and Abbott, 2011; Schuur et al., 2013, 2008, 2009; Zimov et al., 2006). Soil carbon uncertainty leads directly to uncertainties in CO_2 and CH_4 fluxes as the primary carbon source for those fluxes (i.e., Rh for CO_2). Model uncertainty in soil carbon is primarily because the basic paradigm of simple soil carbon modeling is vulnerable to the relatively highly heterogeneous soil physical environments – essentially a scatter of micro-scale frozen or unfrozen environments – some of which favor preservation of organic C much more than others. As such, environmentally determined turnover can vary by orders of magnitude within the top meter of soil. Moreover, most models do not represent well the fast and

BGD
11, 2887–2932, 2014

slow storage and turnover rates of soil carbon with depth. In our analysis, soil carbon typically increased with NPP across the wider Alaskan region: soil carbon increased by 1 $kg\,C\,m^{-2}$ for every 0.02 $kg\,C\,m^{-2}\,yr^{-1}$ increase in NPP ($r^2 = 0.64$; $p < 0.05$), corresponding to a bulk turnover time of 3 yr if in equilibrium. Total soil carbon for Alaska varied from 1.4 to 29.3 $kg\,C\,m^{-2}$ across models. This range of model estimates contrasts with the latest observation-based soil carbon assessments from recent Arctic/Alaska soil carbon syntheses, showing soil carbon ranges from 35–70 $kg\,C\,m^{-2}$ total (Hugelius et al., 2013; Johnson et al., 2011; Mishra and Riley, 2012; Ping et al., 2008; Tarnocai et al., 2009).

A unique feature of our analysis is the comparison of NACP Regional and TRENDY model runs, for which the latter used common forcing data unlike the former. A fundamental question with MIPs is: what is more important – the forcing data or the model physics? TRENDY prescribed historical climate and CO_2 trends to the DGVMs so that the carbon sink/source is caused by local imbalance between GPP and Re, given the residence time of C in pools. NACP, on the other hand, asked modelers to provide their "best regional flux estimates", and many models did not perform any spin up or historical simulations. We might expect TRENDY models to have larger carbon sinks than the NACP models. We also might expect that the TRENDY models would group together given that they shared common forcing data (CRU+NCEP blended product), unlike the NACP Regional models; however, our results show no grouping of TRENDY or NACP models across variables, space, time, and relative values. Thus, for our study, variability in model output was driven primarily by differences in model physics rather than differences in forcing data. This observation may be more rigorously quantified with further analysis (e.g., cluster, geostatistical regression) (Mueller et al., 2011, 2010; Poulter et al., 2011; Yadav et al., 2010).

Our results are applicable to a number of past and current large-scale field campaigns: the Arctic Boundary Layer Expedition (ABLE; NASA), the Boreal Ecosystem-Atmosphere Study (BOREAS; NASA), the Arctic Research of the Composition of the Troposphere from Aircraft and Satellites (ARCTAS; NASA), CARVE (NASA), the Arctic

BGD
11, 2887–2932, 2014

Boreal Vulnerability Experiment (ABoVE; NASA), and the Next Generation Ecological Experiment (NGEE Arctic; US Department of Energy). ABLE integrated ground-based, aircraft, and satellite platforms focusing on characterization of tropospheric chemistry (Harriss et al., 1994). BOREAS was a multi-scale campaign that laid the foundation for much of subsequent work in the region (Sellers et al., 1995, 1997). ARCTAS focused on Arctic atmospheric composition and climate (Jacob et al., 2010). As was previously mentioned, CARVE measures large-scale carbon fluxes and surface controls in Alaska (Miller et al., 2010). ABoVE aims to investigate the role of interactions between climate, permafrost, hydrology, and disturbance in driving ecosystem processes, focusing on Alaska and northwestern Canada (Goetz et al., 2011). NGEE Arctic addresses how permafrost degradation in a warming Arctic (focusing on Alaska), and the associated changes in landscape evolution, hydrology, soil biogeochemical processes, and plant community succession, will affect feedbacks to the climate system (Wullschleger et al., 2011).

All of these campaigns include Alaska as a major region of focus, and encompass overlapping scientific questions that directly build on the uncertainty in the processes represented in the global models of our study. For CARVE, ABoVE, and NGEE Arctic, in particular, these campaigns must sample the geographic regions that encompass both the greatest representativeness and the greatest uncertainties. Our uncertainty maps alone provide a guide for campaign sampling location strategy. The next step to reducing uncertainties is to benchmark the models used in this analysis against the wealth of data that will be generated by CARVE, ABoVE, and NGEE. Our results highlight the delicate source/sink balance of the current Alaskan terrestrial carbon system and its high sensitivity to future climate change.

5 Conclusion

Because of the rapid rate of change in the Arctic as a result of changing global climate, and because of the actual and potential very large feedbacks from the Arctic on cli-

BGD
11, 2887–2932, 2014
Carbon cycle uncertainty in the Alaskan Arctic
J. B. Fisher et al.

mate change, the Arctic is a critically important region not only for study, but also for accurate representations of current and future feedbacks on global carbon cycle and climate dynamics. We presented here the largest ever multi-terrestrial biosphere model assessment of carbon dynamics and associated uncertainties for Alaska and the North Slope, integrating recent TRENDY, WETCHIMP, and NACP Site and Regional Syntheses model intercomparison projects. Spatial and temporal uncertainties in CO_2 fluxes, CH_4 fluxes, and soil carbon stocks were understandably large, and we provide a quantified baseline of those uncertainties for future campaigns, model developments, and climate assessments to reference and build upon. We also evaluate the CO_2 fertilization and climate sensitivities of the Alaskan Arctic carbon cycle, showing that climate uncertainty dominates CO_2 fertilization uncertainty, so much so that this leads to uncertainty in the sign of the carbon sink/source status of the Arctic. Further work should focus not only on reducing climate uncertainty impacts on the Arctic carbon cycle, but also should converge on understanding and estimating the current state of the Arctic carbon cycle.

Supplementary material related to this article is available online at http://www.biogeosciences-discuss.net/11/2887/2014/ bgd-11-2887-2014-supplement.pdf.

Acknowledgements. Part of the research described in this paper was performed for the Carbon in Arctic Reservoirs Vulnerability Experiment (CARVE), an Earth Ventures (EV-1) investigation by the Jet Propulsion Laboratory, California Institute of Technology, under a contract with the National Aeronautics and Space Administration. This work also supports the NASA Arctic Boreal Vulnerability Experiment (ABoVE) and the NASA Terrestrial Ecology Program. Funding to W.C.O. was provided by the US Department of Energy (Terrestrial Ecosystems Program) and NSF by the Office of Polar Programs and the Division of Environmental Biology. J. R. Melton was supported by a NSERC Visiting Postdoctoral Fellowship. Funding to C. Huntingford was provided by the UK NERC ARCC (Arctic Responses to a Changing

BGD
11, 2887–2932, 2014

Climate) programme. R. Grant, F. Hoffman, S. Levis, J. Randerson, D. Ricciuto, G. van der Werf, E. Weng, and S. Zaehle provided model output for ecosys, CLM-CASA, CLM4-CN, CASA-TRANSCOM, LoTEC, CASA-GFED, TECO, and O-CN, respectively. P. Thornton and S. Sitch helped coordinate the NACP Site and TRENDY syntheses, respectively. We thank D. McGuire for comments on the manuscript. Copyright 2014 California Institute of Technology. Government sponsorship acknowledged.

Author contributions.
J. B. Fisher and C. E. Miller formulated idea; J. B. Fisher designed research; J. B. Fisher and M. Sikka performed research; W. C. Oechel provided data; A. Ahlström, A. M. Arain, I. Baker, J. M. Chen, C. Davidson, M. Dietze, B. El-Masri, D. Hayes, C. Huntingford, A. Jain, P. E. Levy, M. R. Lomas, B. Poulter, D. Price, A. K. Sahoo, K. Schaefer, J. Melton, H. Tian, E. Tomelleri, H. Verbeeck, N. Viovy, R. Wania, and N. Zeng provided model output; all authors contributed to the writing of the paper.
The authors declare no conflict of interest.

References

Agarwal, D. A., Humphrey, M., Beekwilder, N. F., Jackson, K. R., Goode, M. M., and van Ingen, C.: A data-centered collaboration portal to support global carbon-flux analysis, Concurrency and Computation: Practice and Experience, 22, 2323–2334, 2010.

Arain, M. A., Yuan, F., and Andrew Black, T.: Soil–plant nitrogen cycling modulated carbon exchanges in a western temperate conifer forest in Canada, Agr. Forest Meteorol., 140, 171–192, 2006.

Baker, I. T., Prihodko, L., Denning, A. S., Goulden, M., Miller, S., and da Rocha, H. R.: Seasonal drought stress in the Amazon: Reconciling models and observations, J. Geophys. Res., 113, G00B01, doi:10.1029/2007jg000644, 2008.

Baldocchi, D.: "Breathing" of the terrestrial biosphere: lessons learned from a global network of carbon dioxide flux measurement systems, Aust. J. Bot., 56, 1–26, 2008.

Belshe, E. F., Schuur, E. A. G., Bolker, B. M., and Bracho, R.: Incorporating spatial heterogeneity created by permafrost thaw into a landscape carbon estimate, J. Geophys. Res.-Biogeo., 117, G01026, doi:10.1111/ele.12164, 2012.

Belshe, E. F., Schuur, E. A. G., and Bolker, B. M.: Tundra ecosystems observed to be CO_2 sources due to differential amplification of the carbon cycle, Ecol. Lett., 16, 1307–1315, 2013.

Billings, W. D., Luken, J. O., Mortensen, D. A., and Peterson, K. M.: Arctic tundra: a source or sink for atmospheric carbon dioxide in a changing environment?, Oecologia, 53, 7–11, 1982.

Burke, E. J., Hartley, I. P., and Jones, C. D.: Uncertainties in the global temperature change caused by carbon release from permafrost thawing, The Cryosphere, 6, 1063–1076, doi:10.5194/tc-6-1063-2012, 2012.

Cess, R. D., Potter, R. D., Zhang, M.-H., Blanchet, J.-P., Chalita, S., Colman, R., Dazlich, D. A., Genio, A. D. d., Dymnikov, V., Galin, V., Jerrett, D., Keup, E., Lacis, A. A., Le Treut, H., Liang, X.-Z., Mahfouf, J.-F., McAvaney, B. J., Meleshko, V. P., Mitchell, J. F. B., Morcrette, J.-J., Norris, P. M., Randall, D. A., Rikus, L., Roeckner, E., Royer, J.-F., Schlese, U., Sheinin, D. A., Slingo, J. M., Sokolov, A. S., Taylor, K. E., Washington, W. M., Wetherald, R. T., and Yagai, I.: Interpretation of snow–climate feedback as produced by 17 General Circulation Models, Science, 253, 888–892, 1991.

Chapin, F. S., Sturm, M., Serreze, M. C., McFadden, J. P., Key, J. R., Lloyd, A. H., McGuire, A. D., Rupp, T. S., Lynch, A. H., Schimel, J. P., Beringer, J., Chapman, W. L., Epstein, H. E., Euskirchen, E. S., Hinzman, L. D., Jia, G., Ping, C.-L., Tape, K. D., Thompson, C. D. C., Walker, D. A., and Welker, J. M.: Role of land-surface changes in Arctic summer warming, Science, 310, 657–660, 2005.

Chapman, W. L. and Walsh, J. E.: Recent variations of sea ice and air temperature in high latitudes, B. Am. Meteorol. Soc., 74, 33–47, 1993.

Chapman, W. L. and Walsh, J. E.: Simulations of Arctic temperature and pressure by global coupled models, J. Climate, 20, 609–632, 2007.

Chen, J. M., Liu, J., Cihlar, J., and Goulden, M. L.: Daily canopy photosynthesis model through temporal and spatial scaling for remote sensing applications, Ecol. Model., 124, 99–119, 1999.

Christensen, T. R., Johansson, T., Åkerman, H. J., Mastepanov, M., Malmer, N., Friborg, T., Crill, P., and Svensson, B. H.: Thawing sub-arctic permafrost: effects on vegetation and methane emissions, Geophys. Res. Lett., 31, L04501, doi:10.1029/2003gl018680, 2004.

Clark, D. B., Mercado, L. M., Sitch, S., Jones, C. D., Gedney, N., Best, M. J., Pryor, M., Rooney, G. G., Essery, R. L. H., Blyth, E., Boucher, O., Harding, R. J., Huntingford, C., and Cox, P. M.: The Joint UK Land Environment Simulator (JULES), model description – Part 2:

BGD
11, 2887–2932, 2014

Carbon fluxes and vegetation dynamics, Geosci. Model Dev., 4, 701–722, doi:10.5194/gmd-4-701-2011, 2011.

Cox, P. M., Pearson, D., Booth, B. B., Friedlingstein, P., Huntingford, C., Jones, C. D., and Luke, C. M.: Sensitivity of tropical carbon to climate change constrained by carbon dioxide variability, Nature, 494, 341–344, 2013.

Cramer, W., Bondeau, A., Woodward, F. I., Prentice, I. C., Betts, R. A., Brovkin, V., Cox, P. M., Fisher, V., Foley, J. A., Friend, A. D., Kucharik, C., Lomas, M. R., Ramankutty, N., Sitch, S., Smith, B., White, A., and Young-Molling, C.: Global response of terrestrial ecosystem structure and function to CO_2 and climate change: results from six dynamic global vegetation models, Glob. Change Biol., 7, 357–373, 2001.

El Maayar, M., Price, D. T., Black, T. A., Humphreys, E. R., and Jork, E. M.: Sensitivity tests of the integrated biosphere simulator to soil and vegetation characteristics in a pacific coastal coniferous forest, Atmos. Ocean, 40, 313–332, 2002.

Friedlingstein, P., Cox, P., Betts, R., Bopp, L., von Bloh, W., Brovkin, V., Cadule, P., Doney, S., Eby, M., Fung, I., Bala, G., John, J., Jones, C., Joos, F., Kato, T., Kawamiya, M., Knorr, W., Lindsay, K., Matthews, H. D., Raddatz, T., Rayner, P., Reick, C., Roeckner, E., Schnitzler, K. G., Schnur, R., Strassmann, K., Weaver, A. J., Yoshikawa, C., and Zeng, N.: Climate-carbon cycle feedback analysis: results from the C4MIP model intercomparison, J. Climate, 19, 3337–3353, 2006.

Goetz, S., Kimball, J., Mack, M., and Kasischke, E.: Scoping Completed for an Experiment to Assess Vulnerability of Arctic and Boreal Ecosystems, Eos Trans. AGU, 92, doi:10.1029/2011eo180002, 2011.

Grant, R. F., Barr, A. G., Black, T. A., Margolis, H. A., Dunn, A. L., Metsaranta, J., Wang, S., McCaughey, J. H., and Bourque, C. A.: Interannual variation in net ecosystem productivity of Canadian forests as affected by regional weather patterns – a Fluxnet-Canada synthesis, Agr. Forest Meteorol., 149, 2022–2039, 2009.

Harriss, R. C., Wofsy, S. C., Hoell, J. M., Jr., Bendura, R. J., Drewry, J. W., McNeal, R. J., Pierce, D., Rabine, V., and Snell, R. L.: The Arctic Boundary Layer Expedition (ABLE-3B): July–August 1990, J. Geophys. Res., 99, 1635–1643, 1994.

Hayes, D. J., McGuire, A. D., Kicklighter, D. W., Gurney, K. R., Burnside, T. J., and Melillo, J. M.: Is the northern high-latitude land-based CO_2 sink weakening?, Global Biogeochem. Cy., 25, GB3018, doi:10.1029/2010GB003813, 2011.

Hayes, D. J., Turner, D. P., Stinson, G., McGuire, A. D., Wei, Y., West, T. O., Heath, L. S., de Jong, B., McConkey, B. G., Birdsey, R. A., Kurz, W. A., Jacobson, A. R., Huntzinger, D. N., Pan, Y., Post, W. M., and Cook, R. B.: Reconciling estimates of the contemporary North American carbon balance among terrestrial biosphere models, atmospheric inversions, and a new approach for estimating net ecosystem exchange from inventory-based data, Glob. Change Biol., 18, 1282–1299, 2012.

Hinzman, L., Bettez, N., Bolton, W., Chapin, F., Dyurgerov, M., Fastie, C., Griffith, B., Hollister, R., Hope, A., Huntington, H., Jensen, A., Jia, G., Jorgenson, T., Kane, D., Klein, D., Kofinas, G., Lynch, A., Lloyd, A., McGuire, A., Nelson, F., Oechel, W., Osterkamp, T., Racine, C., Romanovsky, V., Stone, R., Stow, D., Sturm, M., Tweedie, C., Vourlitis, G., Walker, M., Walker, D., Webber, P., Welker, J., Winker, K., and Yoshikawa, K.: Evidence and implications of recent climate change in northern Alaska and other Arctic regions, Climatic Change, 72, 251–298, 2005.

Hugelius, G., Tarnocai, C., Broll, G., Canadell, J. G., Kuhry, P., and Swanson, D. K.: The Northern Circumpolar Soil Carbon Database: spatially distributed datasets of soil coverage and soil carbon storage in the northern permafrost regions, Earth Syst. Sci. Data, 5, 3–13, doi:10.5194/essd-5-3-2013, 2013.

Huntzinger, D. N., Post, W. M., Wei, Y., Michalak, A. M., West, T. O., Jacobson, A. R., Baker, I. T., Chen, J. M., Davis, K. J., Hayes, D. J., Hoffman, F. M., Jain, A. K., Liu, S., McGuire, A. D., Neilson, R. P., Potter, C., Poulter, B., Price, D., Raczka, B. M., Tian, H. Q., Thornton, P., Tomelleri, E., Viovy, N., Xiao, J., Yuan, W., Zeng, N., Zhao, M., and Cook, R.: North American Carbon Program (NACP) regional interim synthesis: terrestrial biospheric model intercomparison, Ecol. Model., 232, 144–157, 2012.

IPCC: Contribution of Working Group I to the Fourth Assessment Report of the Intergovernmental Panel on Climate Change, in: Climate Change 2007: the Physical Science Basis, edited by: Solomon, S., Qin, D., Manning, M., Chen, Z., Marquis, M., Averyt, K. B., Tignor, M., and Miller, H. L., Cambridge University Press, Cambridge, UK and New York, NY, USA, 2007.

Jacob, D. J., Crawford, J. H., Maring, H., Clarke, A. D., Dibb, J. E., Emmons, L. K., Ferrare, R. A., Hostetler, C. A., Russell, P. B., Singh, H. B., Thompson, A. M., Shaw, G. E., McCauley, E., Pederson, J. R., and Fisher, J. A.: The Arctic Research of the Composition of the Troposphere from Aircraft and Satellites (ARCTAS) mission: design, execution, and first results, Atmos. Chem. Phys., 10, 5191–5212, doi:10.5194/acp-10-5191-2010, 2010.

Jain, A. K. and Yang, X.: Modeling the effects of two different land cover change data sets on the carbon stocks of plants and soils in concert with CO_2 and climate change, Global Biogeochem. Cy., 19, GB2015, doi:10.1029/2004gb002349, 2005.

Johnson, K. D., Harden, J., McGuire, A. D., Bliss, N. B., Bockheim, J. G., Clark, M., Nettleton-Hollingsworth, T., Jorgenson, M. T., Kane, E. S., Mack, M., O'Donnell, J., Ping, C.-L., Schuur, E. A. G., Turetsky, M. R., and Valentine, D. W.: Soil carbon distribution in Alaska in relation to soil-forming factors, Geoderma, 167–168, 71–84, 2011.

Koven, C. D., Ringeval, B., Friedlingstein, P., Ciais, P., Cadule, P., Khvorostyanov, D., Krinner, G., and Tarnocai, C.: Permafrost carbon-climate feedbacks accelerate global warming, P. Natl. Acad. Sci. USA, 108, 14769–14774, 2011.

Krinner, G., Viovy, N., de Noblet-Ducoudré, N., Ogée, J., Polcher, J., Friedlingstein, P., Ciais, P., Sitch, S., and Prentice, C. I.: Evaluation of ecosystem dynamics, plant geography and terrestrial carbon cycling in the LPJ dynamic global vegetation model, Global Biogeochem. Cy., 19, 1–33, 2005.

Kuhry, P., Ping, C.-L., Schuur, E. A. G., Tarnocai, C., and Zimov, S.: Report from the International Permafrost Association: carbon pools in permafrost regions, Permafrost Periglac., 20, 229–234, 2009.

Kwon, H.-J., Oechel, W. C., Zulueta, R. C., and Hastings, S. J.: Effects of climate variability on carbon sequestration among adjacent wet sedge tundra and moist tussock tundra ecosystems, J. Geophys. Res., 111, G03014, doi:10.1029/2005jg000036, 2006.

Levy, P. E., Cannell, M. G. R., and Friend, A. D.: Modelling the impact of future changes in climate, CO_2 concentration and land use on natural ecosystems and the terrestrial carbon sink, Global Environ. Chang., 14, 21–30, 2004.

Mack, M. C., Schuur, E. A. G., Bret-Harte, M. S., Shaver, G. R., and Chapin, F. S.: Ecosystem carbon storage in arctic tundra reduced by long-term nutrient fertilization, Nature, 431, 440–443, 2004.

Marion, G. M. and Oechel, W. C.: Mid- to late-Holocene carbon balance in Arctic Alaska and its implications for future global warming, The Holocene, 3, 193–200, 1993.

McGuire, A. D., Chapin, F. S., Walsh, J. E., and Wirth, C.: Integrated regional changes in Arctic climate feedbacks: implications for the global climate system, Annu. Rev. Env. Resour., 31, 61–91, 2006.

BGD

11, 2887–2932, 2014

McGuire, A. D., Anderson, L. G., Christensen, T. R., Dallimore, S., Guo, L., Hayes, D. J., Heimann, M., Lorenson, T. D., Macdonald, R. W., and Roulet, N.: Sensitivity of the carbon cycle in the Arctic to climate change, Ecol. Monogr., 79, 523–555, 2009.

McGuire, A. D., Christensen, T. R., Hayes, D., Heroult, A., Euskirchen, E., Kimball, J. S., Koven, C., Lafleur, P., Miller, P. A., Oechel, W., Peylin, P., Williams, M., and Yi, Y.: An assessment of the carbon balance of Arctic tundra: comparisons among observations, process models, and atmospheric inversions, Biogeosciences, 9, 3185–3204, doi:10.5194/bg-9-3185-2012, 2012.

Melton, J. R., Wania, R., Hodson, E. L., Poulter, B., Ringeval, B., Spahni, R., Bohn, T., Avis, C. A., Beerling, D. J., Chen, G., Eliseev, A. V., Denisov, S. N., Hopcroft, P. O., Lettenmaier, D. P., Riley, W. J., Singarayer, J. S., Subin, Z. M., Tian, H., Zürcher, S., Brovkin, V., van Bodegom, P. M., Kleinen, T., Yu, Z. C., and Kaplan, J. O.: Present state of global wetland extent and wetland methane modelling: conclusions from a model inter-comparison project (WETCHIMP), Biogeosciences, 10, 753–788, doi:10.5194/bg-10-753-2013, 2013.

Miller, C. E., Dinardo, S. J., and Carve Science Team: CARVE: The Carbon in Arctic Reservoirs Vulnerability Experiment, American Geophysical Union, Fall Meeting 2010, 13–7 December 2010, San Francisco, 2010.

Mishra, U. and Riley, W. J.: Alaskan soil carbon stocks: spatial variability and dependence on environmental factors, Biogeosciences, 9, 3637–3645, doi:10.5194/bg-9-3637-2012, 2012.

Mueller, B., Seneviratne, S. I., Jiménez, C., Corti, T., Hirschi, M., Balsamo, G., Ciais, P., Dirmeyer, P. A., Fisher, J. B., Guo, Z., Jung, M., Maignan, F., McCabe, M. F., Reichle, R. H., Reichstein, M., Rodell, M., Sheffield, J., Teuling, A. J., Wang, K., Wood, E. F., and Zhang, Y.: Evaluation of global observations-based evapotranspiration datasets and IPCC AR4 simulations, Geophys. Res. Lett., 38, L06402, doi:10.1029/2010GL046230, 2011.

Mueller, K. L., Yadav, V., Curtis, P. S., Vogel, C., and Michalak, A. M.: Attributing the variability of eddy-covariance CO_2 flux measurements across temporal scales using geostatistical regression for a mixed northern hardwood forest, Global Biogeochem. Cy., 24, GB3023, doi:10.1029/2009gb003642, 2010.

Natali, S. M., Schuur, E. A. G., and Rubin, R. L.: Increased plant productivity in Alaskan tundra as a result of experimental warming of soil and permafrost, J. Ecol., 100, 488–498, 2012.

Natali, S. M., Schuur, E. A. G., Webb, E. E., Hicks Pries, C. E., and Crummer, K. G.: Permafrost degradation stimulates carbon loss from experimentally warmed tundra, Ecology, 100, 488–498, doi:10.1890/13-0602.1, 2013.

Oechel, W. C. and Vourlitis, G. L.: The effects of climate change land-atmosphere feedbacks in arctic tundra regions, Trends Ecol. Evol., 9, 324–329, 1994.

Oechel, W. C., Hastings, S. J., Vourlrtis, G., Jenkins, M., Riechers, G., and Grulke, N.: Recent change of Arctic tundra ecosystems from a net carbon dioxide sink to a source, Nature, 361, 520–523, 1993.

Oechel, W. C., Vourlitis, G., and Hastings, S. J.: Cold season CO_2 emission from Arctic soils, Global Biogeochem. Cy., 11, 163–172, 1997.

Oechel, W. C., Vourlitis, G. L., Hastings, S. J., Zulueta, R. C., Hinzman, L., and Kane, D.: Acclimation of ecosystem CO_2 exchange in the Alaskan Arctic in response to decadal climate warming, Nature, 406, 978–981, 2000.

Olefeldt, D., Turetsky, M. R., Crill, P. M., and McGuire, A. D.: Environmental and physical controls on northern terrestrial methane emissions across permafrost zones, Glob. Change Biol., 19, 589–603, 2013.

Overpeck, J., Hughen, K., Hardy, D., Bradley, R., Case, R., Douglas, M., Finney, B., Gajewski, K., Jacoby, G., Jennings, A., Lamoureux, S., Lasca, A., MacDonald, G., Moore, J., Retelle, M., Smith, S., Wolfe, A., and Zielinski, G.: Arctic environmental change of the last four centuries, Science, 278, 1251–1256, 1997.

Piao, S., Sitch, S., Ciais, P., Friedlingstein, P., Peylin, P., Wang, X., Ahlström, A., Anav, A., Canadell, J. G., Cong, N., Huntingford, C., Jung, M., Levis, S., Levy, P. E., Li, J., Lin, X., Lomas, M. R., Lu, M., Luo, Y., Ma, Y., Myneni, R. B., Poulter, B., Sun, Z., Wang, T., Viovy, N., Zaehle, S., and Zeng, N.: Evaluation of terrestrial carbon cycle models for their response to climate variability and to CO_2 trends, Glob. Change Biol., 19, 2117–2132, 2013.

Ping, C.-L., Michaelson, G. J., Jorgenson, M. T., Kimble, J. M., Epstein, H., Romanovsky, V. E., and Walker, D. A.: High stocks of soil organic carbon in the North American Arctic region, Nat. Geosci., 1, 615–619, 2008.

Poulter, B., Frank, D. C., Hodson, E. L., and Zimmermann, N. E.: Impacts of land cover and climate data selection on understanding terrestrial carbon dynamics and the CO_2 airborne fraction, Biogeosciences, 8, 2027–2036, doi:10.5194/bg-8-2027-2011, 2011.

Qian, H., Joseph, R., and Zeng, N.: Enhanced terrestrial carbon uptake in the Northern High Latitudes in the 21st century from the Coupled Carbon Cycle Climate Model Intercomparison Project model projections, Glob. Change Biol., 16, 641–656, 2010.

Randerson, J. T., Thompson, M. V., Conway, T. J., Fung, I. Y., and Field, C. B.: The contribution of terrestrial sources and sinks to trends in the seasonal cycle of atmospheric carbon dioxide, Global Biogeochem. Cy., 11, 535–560, 1997.

Randerson, J. T., Hoffman, F. M., Thornton, P. E., Mahowald, N. M., Lindsay, K., Lee, Y.-H., Nevison, C. D., Doney, S. C., Bonan, G., Stöckli, R., Covey, C., Running, S. W., and Fung, I. Y.: Systematic assessment of terrestrial biogeochemistry in coupled climate-carbon models, Glob. Change Biol., 15, 2462–2484, 2009.

Rienecker, M. M., Suarez, M. J., Gelaro, R., Todling, R., Bacmeister, J., Liu, E., Bosilovich, M. G., Schubert, S. D., Takacs, L., Kim, G.-K., Bloom, S., Chen, J., Collins, D., Conaty, A., da Silva, A., Gu, W., Joiner, J., Koster, R. D., Lucchesi, R., Molod, A., Owens, T., Pawson, S., Pegion, P., Redder, C. R., Reichle, R., Robertson, F. R., Ruddick, A. G., Sienkiewicz, M., and Woollen, J.: MERRA: NASA's Modern-Era Retrospective Analysis for Research and Applications, J. Climate, 24, 3624–3648, 2011.

Riley, W. J., Subin, Z. M., Lawrence, D. M., Swenson, S. C., Torn, M. S., Meng, L., Mahowald, N. M., and Hess, P.: Barriers to predicting changes in global terrestrial methane fluxes: analyses using CLM4Me, a methane biogeochemistry model integrated in CESM, Biogeosciences, 8, 1925–1953, doi:10.5194/bg-8-1925-2011, 2011.

Schaefer, K., Collatz, G. J., Tans, P., Denning, A. S., Baker, I., Berry, J., Prihodko, L., Suits, N., and Philpott, A.: Combined Simple Biosphere/Carnegie-Ames-Stanford Approach terrestrial carbon cycle model, J. Geophys. Res., 113, G03034, doi:10.1111/j.1600-0889.2011.00527.x, 2008.

Schaefer, K., Zhang, T., Bruhwiler, L., and Barrett, A. P.: Amount and timing of permafrost carbon release in response to climate warming, Tellus B, 63, 165–180, 2011.

Schaefer, K., Schwalm, C. R., Williams, C., Arain, M. A., Barr, A., Chen, J. M., Davis, K. J., Dimitrov, D., Hilton, T. W., and Hollinger, D. Y.: A model-data comparison of gross primary productivity: Results from the North American Carbon Program site synthesis, J. Geophys. Res. Biogeosci., 117, G03010, doi:10.1029/2012JG001960, 2012.

Schuur, E. A. G. and Abbott, B.: Climate change: high risk of permafrost thaw, Nature, 480, 32–33, 2011.

Schuur, E. A. G., Bockheim, J., Canadell, J. G., Euskirchen, E., Field, C. B., Goryachkin, S. V., Hagemann, S., Kuhry, P., Lafleur, P. M., Lee, H., Mazhitova, G., Nelson, F. E., Rinke, A., Romanovsky, V. E., Shiklomanov, N., Tarnocai, C., Venevsky, S., Vogel, J. G., and Zimov, S. A.:

BGD
11, 2887–2932, 2014

Carbon cycle uncertainty in the Alaskan Arctic

J. B. Fisher et al.

Vulnerability of permafrost carbon to climate change: implications for the global carbon cycle, BioScience, 58, 701–714, 2008.

Schuur, E. A. G., Vogel, J. G., Crummer, K. G., Lee, H., Sickman, J. O., and Osterkamp, T. E.: The effect of permafrost thaw on old carbon release and net carbon exchange from tundra, Nature, 459, 556–559, 2009.

Schuur, E. A. G., Abbott, B. W., Bowden, W. B., Brovkin, V., Camill, P., Canadell, J. G., Chanton, J. P., Chapin III, F. S., Christensen, T. R., Ciais, P., Crosby, B. T., Czimczik, C. I., Grosse, G., Harden, J., Hayes, D. J., Hugelius, G., Jastrow, J. D., Jones, J. B., Kleinen, T., Koven, C. D., Krinner, G., Kuhry, P., Lawrence, D. M., McGuire, A. D., Natali, S. M., O'Donnell, J. A., Ping, C. L., Riley, W. J., Rinke, A., Romanovsky, V. E., Sannel, A. B. K., Schädel, C., Schaefer, K., Sky, J., Subin, Z. M., Tarnocai, C., Turetsky, M. R., Waldrop, M. P., Walter Anthony, K. M., Wickland, K. P., Wilson, C. J., and Zimov, S. A.: Expert assessment of vulnerability of permafrost carbon to climate change, Climatic Change, 119, 359–374, 2013.

Schwalm, C. R., Williams, C. A., Schaefer, K., Anderson, R., Arain, M. A., Baker, I., Barr, A., Black, T. A., Chen, G., Chen, J. M., Ciais, P., Davis, K. J., Desai, A., Dietze, M., Dragoni, D., Fischer, M. L., Flanagan, L. B., Grant, R., Gu, L., Hollinger, D., Izaurralde, R. C., Kucharik, C., Lafleur, P., Law, B. E., Li, L., Li, Z., Liu, S., Lokupitiya, E., Luo, Y., Ma, S., Margolis, H., Matamala, R., McCaughey, H., Monson, R. K., Oechel, W. C., Peng, C., Poulter, B., Price, D. T., Riciutto, D. M., Riley, W., Sahoo, A. K., Sprintsin, M., Sun, J., Tian, H., Tonitto, C., Verbeeck, H., and Verma, S. B.: A model-data intercomparison of CO_2 exchange across North America: results from the North American Carbon Program site synthesis, J. Geophys. Res., 115, G00H05, doi:10.1029/2009jg001229, 2010.

Sellers, P., Hall, F., Margolis, H., Kelly, B., Baldocchi, D., den Hartog, G., Cihlar, J., Ryan, M. G., Goodison, B., Crill, P., Ranson, K. J., Lettenmaier, D., and Wickland, D. E.: The Boreal Ecosystem-Atmosphere Study (BOREAS): an overview and early results from the 1994 field year, B. Am. Meteorol. Soc., 76, 1549–1577, 1995.

Sellers, P. J., Hall, F. G., Kelly, R. D., Black, A., Baldocchi, D., Berry, J., Ryan, M., Ranson, K. J., Crill, P. M., Lettenmaier, D. P., Margolis, H., Cihlar, J., Newcomer, J., Fitzjarrald, D., Jarvis, P. G., Gower, S. T., Halliwell, D., Williams, D., Goodison, B., Wickland, D. E., and Guertin, F. E.: BOREAS in 1997: Experiment overview, scientific results, and future directions, J. Geophys. Res., 102, 28731–28769, 1997.

Serreze, M. C., Walsh, J. E., Chapin, F. S., Osterkamp, T., Dyurgerov, M., Romanovsky, V., Oechel, W. C., Morison, J., Zhang, T., and Barry, R. G.: Observational evidence of recent change in the northern high-latitude environment, Climatic Change, 46, 159–207, 2000.
Sistla, S. A., Moore, J. C., Simpson, R. T., Gough, L., Shaver, G. R., and Schimel, J. P.: Long-term warming restructures Arctic tundra without changing net soil carbon storage, Nature, 497, 615–618, 2013.
Sitch, S., Smith, B., Prentice, C. I., Arneth, A., Bondeau, A., Cramer, W., JKaplan, J. O., Lucht, W., Sykes, M. T., Thonicke, K., and Venevsky, S.: Evaluation of ecosystem dynamics, plant geography and terrestrial carbon cycling in the LPJ dynamic global vegetation model, Glob. Change Biol., 9, 161–185, 2003.
Smith, B., Prentice, I. C., and Sykes, M. T.: Representation of vegetation dynamics in modelling of terrestrial ecosystems: comparing two contrasting approaches within European climate space, Global. Ecol. Biogeogr., 10, 621–637, 2001.
Spahni, R., Wania, R., Neef, L., van Weele, M., Pison, I., Bousquet, P., Frankenberg, C., Foster, P. N., Joos, F., Prentice, I. C., and van Velthoven, P.: Constraining global methane emissions and uptake by ecosystems, Biogeosciences, 8, 1643–1665, doi:10.5194/bg-8-1643-2011, 2011.
Tarnocai, C.: The effect of climate change on carbon in Canadian peatlands, Global Planet. Change, 53, 222–232, 2006.
Tarnocai, C., Canadell, J. G., Schuur, E. A. G., Kuhry, P., Mazhitova, G., and Zimov, S.: Soil organic carbon pools in the northern circumpolar permafrost region, Global Biogeochem. Cy., 23, GB2023, doi:10.1029/2008GB003327, 2009.
Thornton, P. E., Lamarque, J.-F., Rosenbloom, N. A., and Mahowald, N. M.: Influence of carbon-nitrogen cycle coupling on land model response to CO_2 fertilization and climate variability, Global Biogeochem. Cy., 21, 1–15, 2007.
Tian, H., Chen, G., Liu, M., Zhang, C., Sun, G., Lu, C., Xu, X., Ren, W., Pan, S., and Chappelka, A.: Model estimates of net primary productivity, evapotranspiration, and water use efficiency in the terrestrial ecosystems of the southern United States during 1895–2007, Forest Ecol. Manag., 259, 1311–1327, 2010.
van der Werf, G. R., Randerson, J. T., Collatz, G. J., Giglio, L., Kasibhatla, P. S., Arellano, A. F., Olsen, S. C., and Kasischke, E. S.: Continental-scale partitioning of fire emissions during the 1997 to 2001 El Niño/La Niña period, Science, 303, 73–76, 2004.

BGD
11, 2887–2932, 2014

Carbon cycle uncertainty in the Alaskan Arctic

J. B. Fisher et al.

Walsh, J. E., Kattsov, V. M., Chapman, W. L., Govorkova, V., and Pavlova, T.: Comparison of Arctic climate simulations by uncoupled and coupled global models, J. Climate, 15, 1429–1446, 2002.

Wang, T., Ciais, P., Piao, S. L., Ottlé, C., Brender, P., Maignan, F., Arain, A., Cescatti, A., Gianelle, D., Gough, C., Gu, L., Lafleur, P., Laurila, T., Marcolla, B., Margolis, H., Montagnani, L., Moors, E., Saigusa, N., Vesala, T., Wohlfahrt, G., Koven, C., Black, A., Dellwik, E., Don, A., Hollinger, D., Knohl, A., Monson, R., Munger, J., Suyker, A., Varlagin, A., and Verma, S.: Controls on winter ecosystem respiration in temperate and boreal ecosystems, Biogeosciences, 8, 2009–2025, doi:10.5194/bg-8-2009-2011, 2011.

Wania, R., Ross, I., and Prentice, I. C.: Implementation and evaluation of a new methane model within a dynamic global vegetation model: LPJ-WHyMe v1.3.1, Geosci. Model Dev., 3, 565–584, doi:10.5194/gmd-3-565-2010, 2010.

Wania, R., Melton, J. R., Hodson, E. L., Poulter, B., Ringeval, B., Spahni, R., Bohn, T., Avis, C. A., Chen, G., Eliseev, A. V., Hopcroft, P. O., Riley, W. J., Subin, Z. M., Tian, H., van Bodegom, P. M., Kleinen, T., Yu, Z. C., Singarayer, J. S., Zürcher, S., Lettenmaier, D. P., Beerling, D. J., Denisov, S. N., Prigent, C., Papa, F., and Kaplan, J. O.: Present state of global wetland extent and wetland methane modelling: methodology of a model inter-comparison project (WETCHIMP), Geosci. Model Dev., 6, 617–641, doi:10.5194/gmd-6-617-2013, 2013.

Weng, E. and Luo, Y.: Soil hydrological properties regulate grassland ecosystem responses to multifactor global change: a modeling analysis, J. Geophys. Res., 113, G03003, doi:10.1029/2007jg000539, 2008.

Wullschleger, S. D., Hinzman, L. D., and Wilson, C. J.: Planning the Next Generation of Arctic Ecosystem Experiments, Eos Trans. AGU, 92, doi:10.1029/2011eo170006, 2011.

Xue, Y., Sellers, P. J., Kinter, J. L., and Shukla, J.: A simplified biosphere model for global climate studies, J. Climate, 4, 345–364, 1991.

Yadav, V., Mueller, K. L., Dragoni, D., and Michalak, A. M.: A geostatistical synthesis study of factors affecting gross primary productivity in various ecosystems of North America, Biogeosciences, 7, 2655–2671, doi:10.5194/bg-7-2655-2010, 2010.

Zaehle, S., Friend, A. D., Friedlingstein, P., Dentener, F., Peylin, P., and Schulz, M.: Carbon and nitrogen cycle dynamics in the O-CN land surface model, II: The role of the nitrogen cycle in the historical terrestrial C balance, Global Biogeochem. Cy., 24, 1–14, 2010.

BGD

11, 2887–2932, 2014

Zeng, N., Qian, H., Roedenbeck, C., and Heimann, M.: Impact of 1998–2002 midlatitude drought and warming on terrestrial ecosystem and the global carbon cycle, Geophys. Res. Lett., 32, L22709, doi:10.1029/2005gl024607, 2005.

Zhao, M. S., Heinsch, F. A., Nemani, R. R., and Running, S. W.: Improvements of the MODIS terrestrial gross and net primary production global data set, Remote Sens. Environ., 98, 164–176, 2005.

Zimov, S. A., Schuur, E. A. G., and Chapin, F. S.: Permafrost and the global carbon budget, Science, 312, 1612–1613, 2006.

Table 1. Models and carbon output variables.

	NEE	GPP	Re	Rh	Ra	NPP	Csoil	CH_4
			NACP Regional					
BEPS	√	√	√	√	√	√		
Can-IBIS	√	√	√	√	√	√	√	
CASA-GFED	√	√	√					
CASA-TRANSCOM	√							
CLM-CASA	√	√	√	√	√	√	√	
CLM4-CN	√	√	√	√	√	√	√	
DLEM	√	√	√	√	√	√	√	
ISAM	√			√		√		
LPJwsl	√	√	√	√	√	√	√	
MOD17	√	√	√					
ORCHIDEE	√	√	√	√	√	√		
SiB3	√	√	√	√	√	√		
TEM6	√	√	√	√	√	√	√	
VEGAS2	√	√	√	√	√	√		
			TRENDY					
CLM4-CN	√	√	√	√	√	√	√	
HYLAND	√	√	√	√	√	√	√	
LPJwsl	√	√	√	√	√	√	√	
LPJ-GUESS	√	√	√	√	√	√	√	
OCN	√	√	√	√	√	√	√	
ORCHIDEE	√	√	√	√	√	√	√	
SDGVM	√	√	√	√	√	√	√	
TRIFFID	√	√	√	√	√	√	√	
VEGAS	√	√	√	√	√	√	√	

Table 1. Continued.

	NEE	GPP	Re	Rh	Ra	NPP	Csoil	CH_4
WETCHIMP								
CLM4Me								√
DLEM								√
LPJ-Bern								√
LPJ-WhyMe								√
LPJwsl								√
ORCHIDEE								√
SDGVM								√
NACP Site								
In situ (ATQ, BRW)	√	√	√					
Can-IBIS	√	√	√				√	
CN-CLASS	√	√	√				√	
DLEM	√	√	√				√	
Ecosys	√	√	√				√	
LPJwsl	√	√	√				√	
ORCHIDEE	√	√	√				√	
SiB	√	√	√					
SiBCASA	√	√	√				√	
SSiB2	√	√	√					
TECO	√	√	√				√	

Notes: NEE includes NBP (all TRENDY models except HYLAND) and NEP (NACP Regional: BEPS, Can-IBIS, CLM-CASA, CLM4-CN, VEGAS2; TRENDY: HYLAND). Re may be calculated from Rh + Ra (e.g., NACP Regional) or NEE-GPP (all NACP Regional except CASA-TRANSCOM and ISAM; all TRENDY). Ra may be calculated from NEE-GPP-Rh (NACP Regional: BEPS, CLM-CASA, CLM4-CN, ORCHIDEE, TEM6; TRENDY: HYLAND, ORCHIDEE, VEGAS). NPP may be calculated from GPP-Ra (TRENDY: LPJ-GUESS).

Fig. 1. Map of the Alaskan Arctic North Slope delineation, and the two AmeriFlux sites used in this study (Atqasuk: ATQ; Barrow: BRW).

BGD
11, 2887–2932, 2014

Title Page
Abstract | Introduction
Conclusions | References
Tables | Figures
◀| |▶
◀ ▶
Back | Close
Full Screen / Esc
Printer-friendly Version
Interactive Discussion

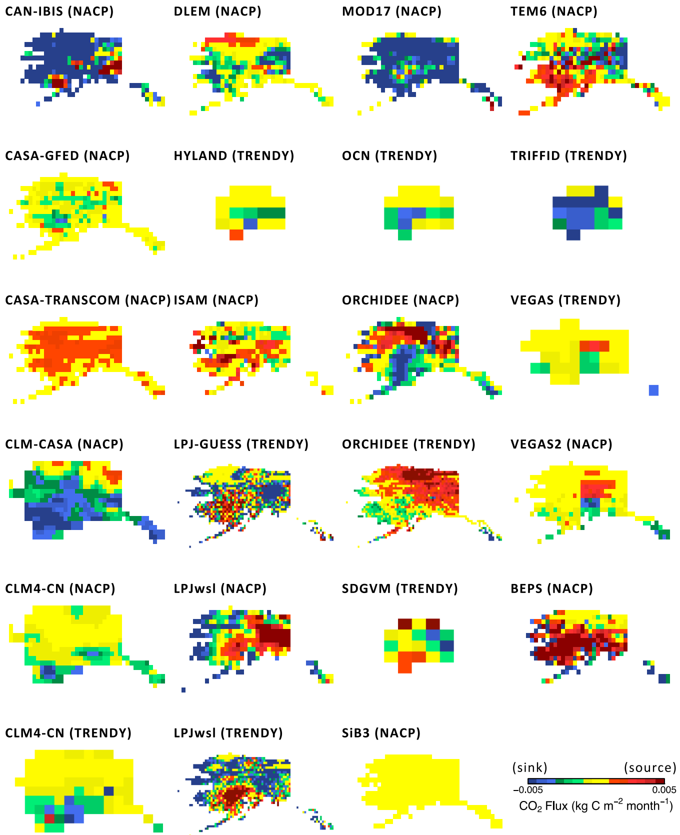

Fig. 2. Mean annual (2003) net CO_2 flux for Alaska. Model output was part of the TRENDY (common forcing) and NACP Regional (variable forcing) syntheses.

BGD
11, 2887–2932, 2014

Carbon cycle uncertainty in the Alaskan Arctic

J. B. Fisher et al.

Title Page
Abstract | Introduction
Conclusions | References
Tables | Figures
◀| |▶
◀ ▶
Back | Close
Full Screen / Esc
Printer-friendly Version
Interactive Discussion

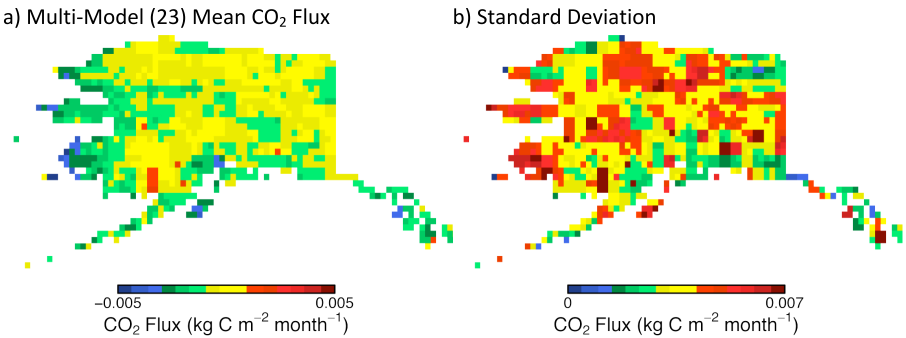

Fig. 3. NACP and TRENDY multi-model ($n = 23$) net CO_2 flux for 2003 **(a)** mean, and **(b)** standard deviation.

BGD
11, 2887–2932, 2014

Carbon cycle uncertainty in the Alaskan Arctic

J. B. Fisher et al.

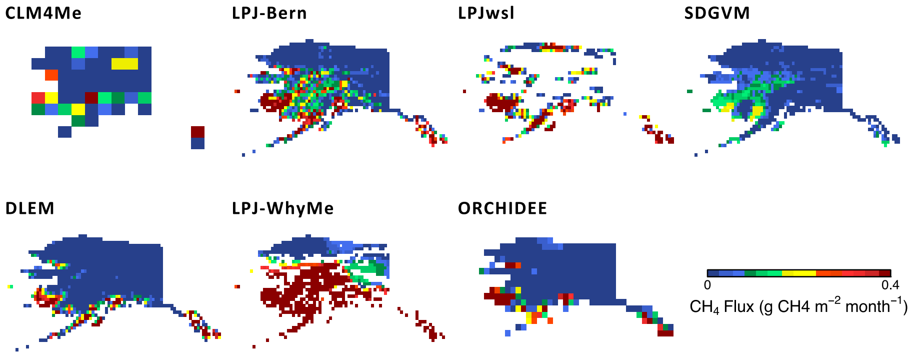

Fig. 4. Mean annual (2003) net CH_4 flux for Alaska. Model output was part of the WETCHIMP model intercomparison project.

BGD
11, 2887–2932, 2014

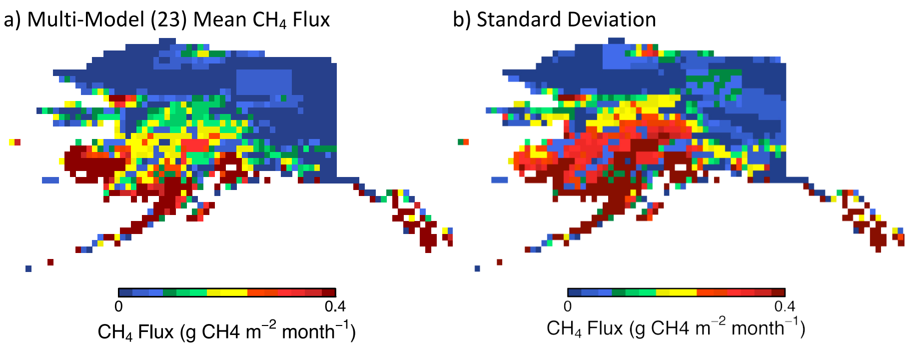

Fig. 5. WETCHIMP multi-model (n = 7) net CH_4 flux for 2003 **(a)** mean, and **(b)** standard deviation.

BGD
11, 2887–2932, 2014

Carbon cycle uncertainty in the Alaskan Arctic

J. B. Fisher et al.

Title Page
Abstract | Introduction
Conclusions | References
Tables | Figures
Back | Close
Full Screen / Esc
Printer-friendly Version
Interactive Discussion

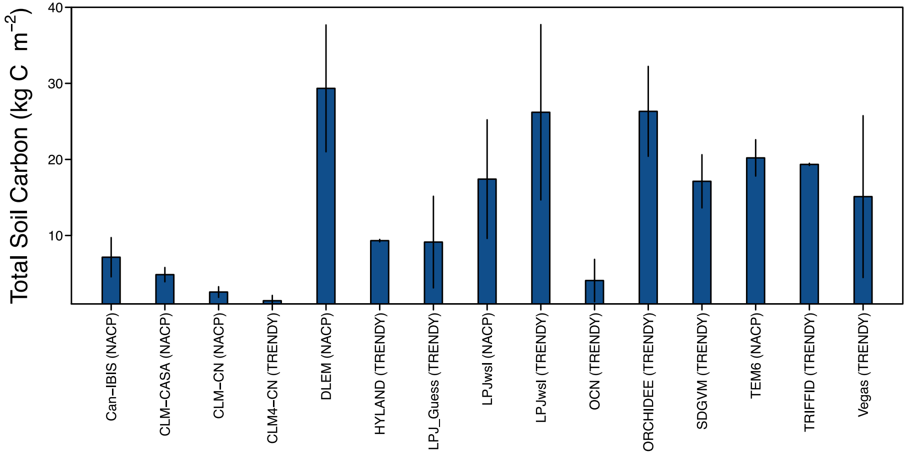

Fig. 6. Mean annual Alaskan Arctic total soil carbon with spatial standard deviations.

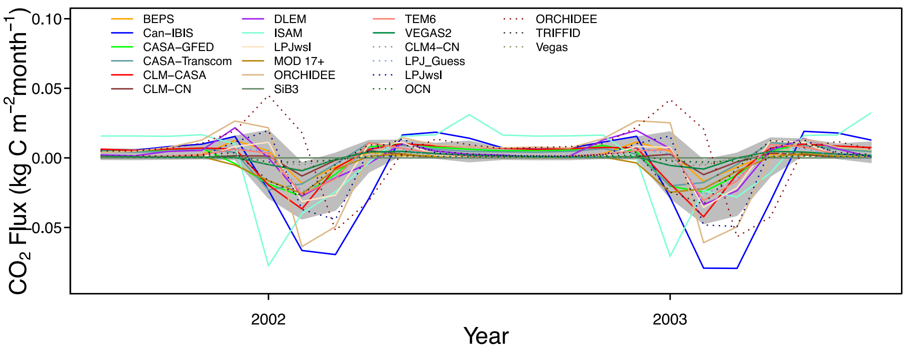

Fig. 7. Mean monthly net CO_2 flux for the Alaskan Arctic for 2002–2003. NACP models are shown as solid lines, and TRENDY models as dashed lines. The gray area is the multi-model standard deviation.

BGD
11, 2887–2932, 2014

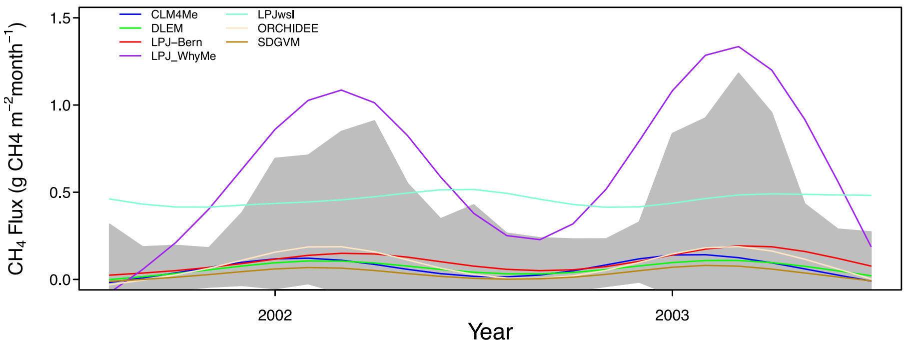

Fig. 8. Mean monthly net CH_4 flux for the Alaskan Arctic for 2002–2003. The gray area is the multi-model standard deviation.

BGD
11, 2887–2932, 2014

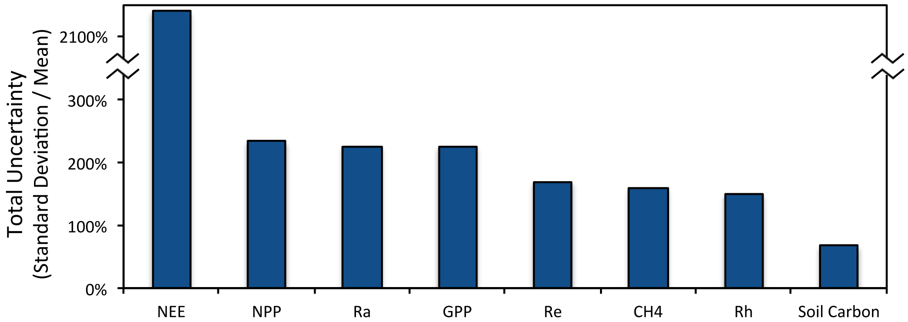

Fig. 9. Total absolute uncertainty (standard deviation/mean) for all carbon components in the Alaskan Arctic, ranked in order from most to least uncertain: (1) net ecosystem exchange (NEE) of CO_2 between land and atmosphere; (2) net primary production (NPP); (3) autotrophic respiration (Ra); (4) gross primary production (GPP); (5) total ecosystem respiration (Re); (6) CH_4 flux; (7) heterotrophic respiration (Rh); and, (8) soil carbon.

BGD
11, 2887–2932, 2014

Carbon cycle uncertainty in the Alaskan Arctic

J. B. Fisher et al.

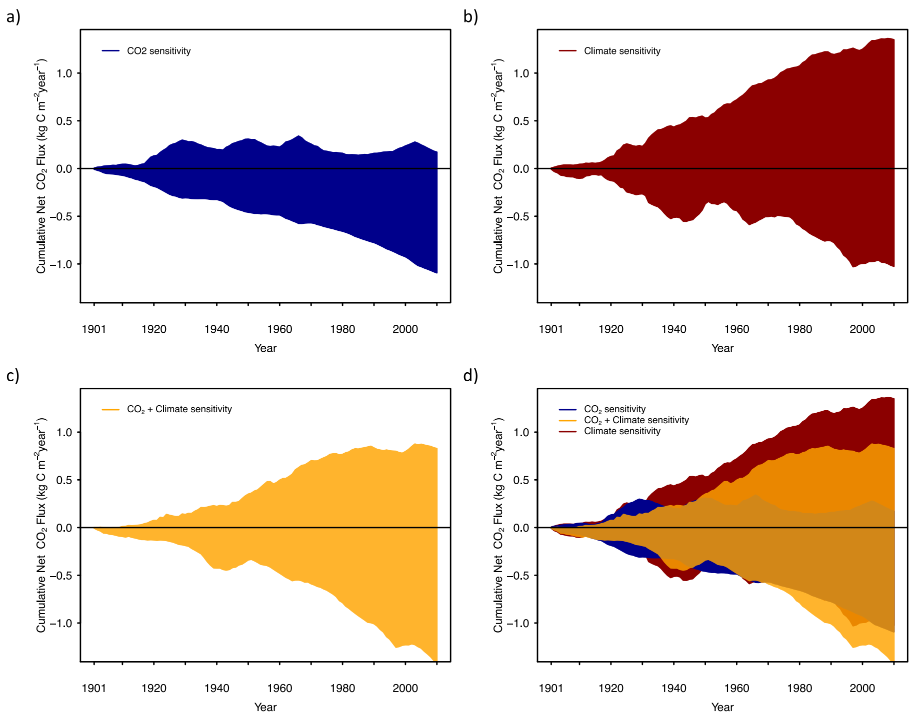

Fig. 10. Feedback/sensitivity analysis for the Alaskan Arctic showing the multi-model ($n = 9$; TRENDY) standard deviation of net CO_2 flux accumulation over the 20th century for: **(a)** CO_2 fertilization alone (β); **(b)** climate impact alone (γ); **(c)** the combined impact of β and γ; and, **(d)** all three feedbacks overlain for visual comparison.

BGD
11, 2887–2932, 2014

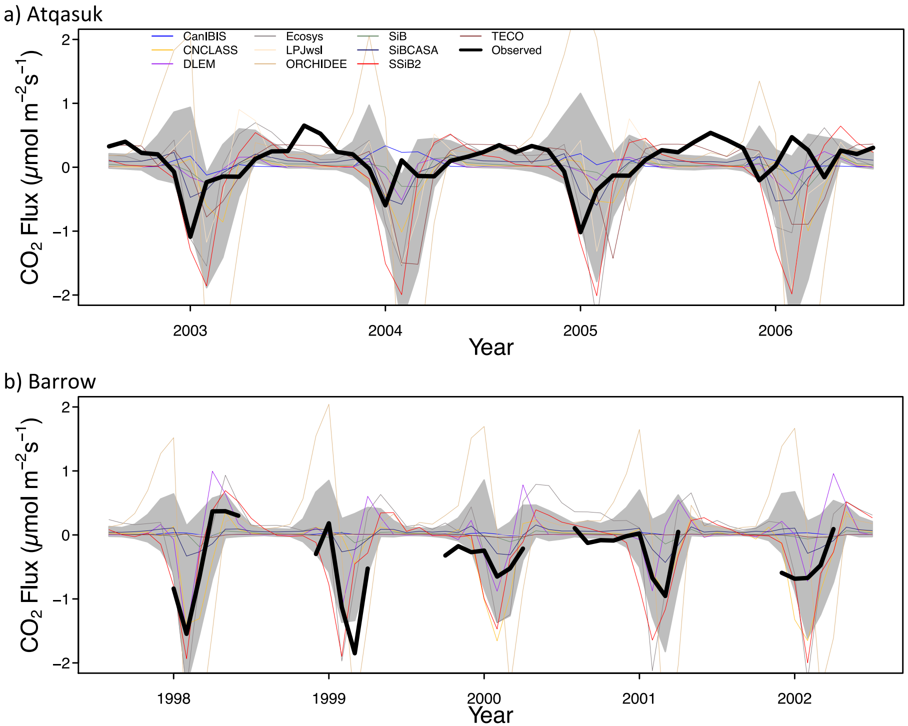

Fig. 11. Mean monthly net CO_2 flux for two sites in the Alaskan Arctic: **(a)** Atqasuk, and **(b)** Barrow. The gray area is the multi-model standard deviation.

BGD
11, 2887–2932, 2014
Carbon cycle uncertainty in the Alaskan Arctic
J. B. Fisher et al.

Title Page
Abstract Introduction
Conclusions References
Tables Figures
◀◀ ▶▶
◀ ▶
Back Close
Full Screen / Esc
Printer-friendly Version
Interactive Discussion